Published in final edited form as:
J Orthop Res. 2014 August ; 32(8): 1052–1060. doi:10.1002/jor.22634.

In Vivo Loss of Cement-Bone Interlock Reduces Fixation Strength in Total Knee Arthroplasties

Jacklyn R. Goodheart, **Mark A. Miller**, and **Kenneth A. Mann**
Department of Orthopedic Surgery, State University of New York, Upstate Medical University, 3216 IHP, 750 East Adams Street, Syracuse, New York, 13210, USA

Jacklyn R. Goodheart: goodheaj@upstate.edu; Mark A. Miller: millerm@upstate.edu; Kenneth A. Mann: mannk@upstate.edu

Abstract

Prevention of aseptic loosening of total knee arthroplasties (TKAs) remains an important clinical challenge. Understanding how changes in morphology at the implant-bone interface with *in vivo* service affects implant stability and strength could lead to new approaches to mitigate loosening. *Enbloc* TKA retrievals and freshly-cemented TKA tibial components were used to determine if the mechanical strength of the interface depended on the amount of cement-bone interlock and the morphology of the supporting bone under the cement layer. Implants were sectioned into small specimens of the cement-interface-bone from under the tibial tray. Micro-CT scans were used to document interlock morphology and architecture of the supporting trabecular bone. Axial compression tests were used to assess mechanical behavior. Postmortem retrievals had lower contact fraction (42±55%) compared to freshly-cemented constructs (121±61%) (p=0.0008). Supporting bone architecture parameters were not different for the two groups. Increased interface contact fraction and supporting bone volume fraction (BV/TV) were positive predictors of interface strength (r^2=0.72, p=0.0001). For the same supporting bone BV/TV, postmortem specimens had weaker interfaces; they were also more compliant. Cemented TKA with *in vivo* service experience a loss of fixation strength and increased micro-motion due to the loss of cement-bone interlock.

Keywords

knee replacement; loosening; interface mechanics; bone resorption; PMMA cement

Introduction

Use of total knee arthroplasty (TKA) worldwide continues to grow at a remarkable rate. In a recent survey of TKA utilization in 18 developed countries, over 1.3 million primary and revision knees were placed in one year, with an annual growth rate of 5 to 17% (1). TKA is a very successful procedure with substantial improvement in patient functional status and quality of life; about 70 to 85% of patients are very satisfied with the results of their surgery

Correspondence: Kenneth A. Mann, PhD., 3216 Institute for Human Performance, SUNY Upstate Medical University, 750 East Adams Street, Syracuse, New York 13210, 1-315-464-9963 (P), 1-315-464-6638 (F), mannk@upstate.edu.

(2). However, the lifetime risk of needing a revision knee replacement has been estimated to be 14.9% for males and 17.4% for females (3). Aseptic loosening continues to be the leading cause of revision (4; 5) with the tibial component as the most common component to loosen.

For cemented tibial components, progressive radiolucencies at the interface between implant and bone correlates with component migration and eventual clinical loosening (6). There is also a transient loss of bone mineral density (BMD) below the tray (7) and some evidence that there is continued loss of BMD over the longer term (8). However, a linkage between the supporting bone BMD and component migration has not been found for cemented tibial components (9). This suggests that morphological changes at the fixation interface between bone and cement after implantation may be responsible for component migration.

Using a series of functioning postmortem-retrieved tibial components, our research group recently developed a method to assess the changes in interlock morphology between bone and cement due to bony remodeling with *in vivo* service (10). During cementation, doughy PMMA flows around trabeculae and leaves a mold in the shape of the interdigitated trabeculae when the cement polymerizes. With *in vivo* service, the interlocked trabeculae may resorb, leaving cavities in the cement layer, and these cavtities indicate locations where the trabeculae originally existed. For a series of 14 postmortem retrievals of cemented tibial components, there was a 75% loss of trabecular interlock in the cement mantle with 10 years of service (11). These dramatic morphologic changes to the implant interface could influence fixation strength of the interface and the loosening of tibial components.

The goal of the present study was to determine if the loss of trabecular interlock that occurs with *in vivo* service results in functionally weaker interfaces. We quantified the interface morphology, supporting trabecular architecture, and mechanical response of cement-bone interface specimens obtained from *enbloc* retrieved tibial components and tibial components that did not have any bony remodeling. We asked two research questions: (2) Does the mechanical strength of the interface depend on the amount of interlock between cement and bone, and the quantity of supporting bone under the cement layer? (3) Do postmortem retrieval specimens have diminished mechanical properties compared to freshly-cemented specimens even with the same quantity of supporting bone?

Methods

Specimen Preparation

Twenty-two fresh-frozen cadaver knees were obtained from the Anatomical Gift Programs at SUNY Upstate Medical University (Syracuse, NY). Eleven knees had total knee replacements (TKR) with radiographically well-fixed cemented tibial components; these were used to create specimens for the postmortem retrieval group (Table 1). The retrievals all had metal trays with stems and had time in service ranging from 1 to 20 years. Eleven cadaver proximal tibiae (matched by age and sex to the postmortem retrieval group) without implants were used to create specimens for the freshly-cemented group, where there was no remodeling of the bone. The freshly-cemented group represented the morphological state at the completion of surgery. The freshly-cemented specimens were created in the lab (21° C) using an approach that simulated the intra-operative environment. Proximal tibiae were

stripped of soft tissue and warmed to 37° C in a simulated blood analog solution (12). A trans-axial cut of the proximal tibia was made followed by pulsatile lavage of the cut bone surface. Cement (Simplex P, Stryker Orthopaedics, Mahwah, NJ, USA) was applied to the bone surface in a doughy state using digital pressure and a pressing motion with a spatula to press the cement into the trabecular bone bed prior to placement of the tibial tray.

Mechanical test specimens containing the cement, cement-bone interface, and supporting trabecular bone bed were taken from medial and lateral regions of the tibial tray, 20–30mm from the central axis of the implant. This corresponded to regions below the center of the femoral condyles. The specimens were cut using a water irrigated high-speed silicon carbide saw (Isomet 2000, Buehler Inc., Lake Bluff, IL, USA). Cuboid shaped cement-bone specimens were created from the underside of the tibial tray with cross sections of ~8mm×8mm (Figure 1). For cases where the interface did not appear to have substantial interlock between cement and bone, supporting acrylic side plates were attached to prevent damage to the interface during preparation. Two medial and two lateral specimens were taken from each tibia, resulting in a total of 44 postmortem retrieval and 44 freshly-cemented specimens.

Supporting Trabecular Bone Architecture and Interface Morphology

All specimens were scanned with a micro-computed tomography (micro-CT) scanner at 16 μm resolution (Scanco Inc. Media, PA, USA) to document cement and bone morphology. Trabecular architecture was characterized for a 5 mm zone immediately distal to the cement layer (Figure 1). A purification procedure (1 voxel erosion-dilation and region growing with 6-point connectivity) was used to identify the trabecular bone and remove spurious debris from the cutting operation. Three-dimensional morphology measurements were made using the Scanco trabecular bone architecture software and included the trabecular bone volume fraction (BV/TV), connectivity density (Conn.D), structural model index (SMI), trabecular thickness (Tb.Th), trabecular spacing (Tb.Sp), degree of anisotropy (DA), and bone tissue density. A lower cut-off threshold of 467.1 mg/cc was used to segment the bone tissue.

The *contact fraction* at the interface between the cement and bone was calculated using a stereology method (ImageJ, ImageJ.NIH.gov) where 100 grid-lines in were projected perpendicular (relative to the transverse cut) to the interface of the micro-CT images. Points of cement-bone contact were counted and divided by the total number of projection lines to determine contact fraction. The *interdigitation depth* was determined from the CT scan sets by measuring the axial distance from the distal extent of cement penetration into the trabecular bone to the proximal extent of existing bone penetration into the cement. This measure was made in four quadrants using the transaxial CT slices; the interdigitation depth measurements from the four quadrants were averaged to give one interdigitation depth measure for each specimen. To estimate the *initial interdigitation depth* of the postmortem retrievals, the axial distance from the distal extent of cement penetration into the trabecular bone to the proximal extent of the cement mold was measured.

Biomechanical Testing

The test specimens were fixed to grips of a mechanical test frame (QTest, MTS Systems Corp, Eden Prarie, MN, USA) using PMMA cement (see Figure 1) While the cement cured, the specimens were hydrated with a buffered saline solution. Prior to testing, any supporting acrylic side plates were severed with a hot scalpel blade. Uniaxial compression tests were performed in laboratory air at room temperature under displacement control at 1 mm/min. Loading was applied in compression until there was a 20% drop in applied force from the peak. A 2 mega-pixel imaging system with telecentric lens was used to capture the failure process during loading. Two-dimensional digital image correlation (DIC) (MatchID, Cathloic University College Ghent, Belgium) was used to document the local deformation of the cement, cement-bone interface, and bone regions (13). For all specimens, the resulting load-displacement curves were converted to apparent stress (force divided by cross sectional area) versus apparent strain (displacement divided by total specimen length) curves. The DIC strain calculations for the cement and bone components were based on the initial ‘gage’ length of that particular component. Strain calculation for the interface was based on a gage length of 1 mm because the interface has no defined thickness. The primary outcome measures of the mechanical tests were the apparent strength (peak apparent stress), energy to failure (area under stress-strain curve), and effective modulus (slope of the pre-yield stress-strain curve). Finally, the fracture location was identified from the strain localization pattern in the bone via DIC, and the distance from the cement-bone interface to the fracture location was measured.

Statistical Analysis

To assess differences in the cement-bone interface morphology and trabecular bone architecture for the freshly-cemented and postmortem retrieval specimens, two sample t-tests were used with Bonferroni correction for multiple comparisons (14). For research question 1, a multiple linear regression model with compressive strength as the dependent variable and cement-bone interface contact fraction and supporting trabecular bone volume fraction (BV/TV) as independent variables was performed. All specimens were pooled as one group. For research question 2, Analysis of Covariance (ANCOVA) was used to determine if the mechanical behavior was different for postmortem and freshly-cemented specimens, using supporting bone volume fraction (BV/TV) as the covariate.

Results

General Morphologic and Biomechanical Behavior

The freshly-cemented specimens (without bone remodeling) exhibited good interlock between cement and bone (Figure 2a–b). In contrast, the postmortem retrieval specimens often exhibited substantial bony resorption (Figure 2c–d) as evidenced by the empty cavities in the cement layer that displayed a regular trabecular pattern. Representative mechanical responses to compressive loading shows that the freshly-cemented specimens (Figure 3a) have small strains in the cement and at the cement-bone interface compared to the supporting trabecular bone. The postmortem retrieval specimens with substantial remaining interlock (Figure 3b) exhibited a mechanical response that was similar to the freshly-cemented specimens. In contrast, postmortem retrieval specimens with substantial trabecular

resorption (Figure 3c) had more interface micro-motion (60 μm), while the behavior of the supporting bone bed remained similar to the cases with good interlock at the cement-bone interface. Finally, postmortem retrieval specimens with little or no interlock and fibrous tissue between the cement and bone (Figure 3d) had substantial micro-motion (1.6 mm) at the cement-bone interface. However, the supporting bone could be very robust, with very high compressive strengths. Failure of the supporting bone occurred closer to the interface for the postmortem retrieval (3.8±2.5 mm) compared to the freshly-cemented specimens (5.8±3.3 mm) (unpaired t-test, p=0.0027).

Morphology of the Cement-bone Interface and Trabecular Bone Architecture

The contact fraction at the cement-bone interface (Table 2) was much smaller (p=0.0008) for the postmortem retrievals (42±55%) when compared to the freshly-cemented specimens (121±61%). The interdigitation depth of trabecular bone into the cement layer for the postmortem specimens (1.8±1.3 mm) was also smaller (p=0.0008) than the freshly-cemented specimens (2.9±1.8 mm). The estimated original interdigitation depth for the postmortem specimens was 2.5±1.1 mm, which was similar to the lab-prepared specimens. While there were large differences in the amount of interlock between cement and bone, none of the architectural parameters for the supporting trabecular bone bed were different between the two groups (Table 2). For example, the bone volume fraction (BV/TV) was similar (p=0.736) for the postmortem specimens (0.118±0.069) and freshly-cemented specimens (0.113±0.051).

Interlock Morphology and Supporting Bone Architecture Influence Mechanical Strength

Specimens with greater contact fraction and bone volume fraction had greater strengths as tested using a two-parameter linear regression model (Table 3). A contour plot (Figure 4) illustrates the distribution of postmortem retrieval and freshly-cemented specimens over the BV/TV versus interface contact fraction space, and how these are related to interface strength.

Effect of In Vivo Service on Mechanical Properties

The strength-BV/TV and modulus-BV/TV relationships were significantly (p<0.0001) different (different slopes) for freshly-cemented and postmortem retrieval specimens (Figure 5A & 5B). For the same quantity of supporting bone under the tibial tray, the postmortem specimens were weaker and more compliant than the freshly-cemented specimens. The energy to break was positively correlated with supporting bone BV/TV (p<0.0001), but there was not a difference in response for the freshly-cemented and postmortem retrievals (Figure 5C). The ANCOVA model parameters are shown in Table 4.

Discussion

Loosening of the cemented tibial component of total knee arthroplasty has been observed clinically, but the changes that occur at the cement-bone interface are generally limited to examination of changes in radiolucencies at this interface. Recent postmortem retrieval work of functioning TKA components has shown that there is resorption of trabeculae that initially interlock with the cement (11), but how this resorption affects the mechanical

integrity of the interface has not been explored. Using a series of postmortem retrievals and age/sex-matched freshly-cemented tibial components, we found that the cement-bone interface is weaker and more compliant for the postmortem retrievals. Further, we found that specimens with less supporting bone and less interlock between cement and bone had weaker interfaces.

This study has several limitations. The sample population of postmortem retrievals used in this study was from our Anatomical Gift Program with different implant types and different surgical techniques including the amount of cement used and degree of pressurization during surgical insertion. However, all tibial components were metal-backed with stems and the resulting interlock structure between the cement and bone was quantified and used as a variable in this study. The freshly-cemented constructs created here may not fully represent the population of osteoarthritic patients that would be candidates for TKA, including cases where there is dense sclerotic bone. However, the postmortem retrievals and freshly-cemented specimens had similar estimated interdigitation depths of cement into the bone bed, suggesting that the initial state of fixation was similar for the two sample populations.

The morphology of the cement-bone interlock region for the postmortem retrievals varied considerably by donor. For example, one postmortem retrieval had substantial remaining interlock (e.g. Fig 3B, 61YO male, 5 years service) and was similar to the freshly-cemented constructs. In contrast, another postmortem retrieval (e.g. Fig 3D, 74YO female, 9 years in service) had complete loss of interlock with development of an intervening fibrous tissue layer. As has been reported previously (11), the amount of interlock between cement and bone has been shown to diminish with longer time in service, but additional factors such as the amount of initial interlock, donor age, sex, and activity level all may contribute to the rate at which the interlocked bone resorbs. A larger sample population could be used to explore these factors.

While there were substantial differences in the amount of cement-bone interlock between the postmortem retrieval and freshly-cemented groups, the architecture of the supporting bone was not significantly different for two groups. There was a trend for decreasing bone volume fraction (BV/TV) and increasing rod-like structures (larger SMI) with increasing donor age and implant time in service. There were also outliers in the postmortem retrieval group (high BV/TV, plate-like morphology with low SMI) for cases where there was a dense layer of bone at the interface and no interlock between cement and bone. Chen and coauthors (15) have reported decreases in BV/TV from middle age (females: 57–68 years, BV/TV=0.22) to elderly (females: 87–98 years, BV/TV=0.18), indicating that BV/TV may reduce at a rate of 0.013/decade. Further work with a much larger set of postmortem retrievals would be useful to explore the role of time in service and donor age on trabecular architecture beneath the tibial component. The Chen group (15) BV/TV measurements were made for regions immediately distal to the subchondral bone, whereas the current trabecular morphology measurements were made approximately 10–15mm below the subchondral bone. This would explain the discrepancy of BV/TV magnitudes between the two studies, as BV/TV decreases moving distally from subchondral bone in the tibia.

The mechanical strength of the interface was correlated to the quantity of supporting bone under the cement layer and the amount of interlock between cement and bone using a two-parameter regression model. From a mechanics perspective this is reasonable as compressive loads must pass from the cement layer, through the interface, to the supporting trabecular bone bed (16). An interface with reduced interlock and lower quantity of trabecular bone could contribute to both a weaker and more compliant specimen. The location of failure in the trabecular bone was closer to the interface for the postmortem retrievals suggesting that changes to the interlock morphology at the interface may contribute to the local failure process. The relationship between interface strength and the amount of interlock has been investigated extensively (17–21), but this is usually performed using lab-prepared specimens with no bone remodeling, and has only been studied in a limited fashion using postmortem retrievals (22).

The postmortem retrieval specimens have diminished compressive strength and increased compliance compared to the freshly-cemented specimens, after accounting for the quantity of supporting bone below the cement-bone interface. This finding indicates that even without changes to the quantity of trabecular bone below the interface, there will be a loss of fixation strength at the cement-bone interface with *in vivo* service. Gebert de Uhlenbrock and coworkers (22) have shown, using a series of postmortem retrieved tibial components, that the tensile force required to pull metal tibial trays off of the proximal tibia decreased with time in service. They also found a shift in the failure mode from the implant-cement interface to the cement-bone interface with time *in vivo* and suggested that the cement-bone interface may become weaker with time in service.

The finding that there is loss of trabecular interlock with cement below tibial trays has only been recently explored. The loss of interlock for cemented tibial components is related to time in service (11) with a loss of interdigitation depth of 25% at 1–2 years, reaching a loss of interdigitation depth of 75% at 10 years in service. Contact between bone and cement with 10 or more years of service was only 6.2% of the interface length. Further, constructs that started with more interlock (~3 mm) also maintained more interlock with *in vivo* service.

Preventing trabecular resorption from the cement-bone interlock regions from occurring also would seem to be an important clinical goal. An improved understanding of the biologic mechanism responsible for the resorption the interlocked trabeculae could lead to new biomaterial or pharmacologic approaches to maintain implant fixation for cemented implants. Possible candidate mechanisms to explain this resorption phenomenon include trabecular stress shielding of the interlocked bone, a local-low pH environment (23), osteolysis due to fluid pumping along the interface (24), or particle induced osteolysis (25).

The results from this study have implications for clinical practice. The loss of interlock between cement and bone with *in vivo* service results in weaker and more compliant interfaces, but the loss of interlock would be difficult to detect with radiographs or even clinical CT scans. The original working rationale for maintaining ~3mm of interdigitation (26) was that there would be cement interlock with at least two transverse trabeculae, and this would provide strength and a platform for load transfer from the cement to the bone.

However, perhaps the '3 mm rule' on interdigitation has an additional benefit. Creating more initial interlock between cement and bone, via adequate bone bed preparation and cement pressurization (~3mm), with the acknowledgement that there will be some loss of interlock with *in vivo* service, could also maintain component interface strength over the long term. The reduction of fixation strength that accompanies the *in vivo* loss of interlock reported here could also represent the initial event that occurs prior to increased interface micro-motion, formation of fibrous tissue, and progressive radiolucencies at the cement-bone interface.

Acknowledgments

The research reported in this publication was supported by the National Institute of Arthritis and Musculoskeletal and Skin Diseases of the National Institutes of Health under Award Number AR42017. The content is solely the responsibility of the authors and does not necessarily represent the official views of the National Institutes of Health. The authors would like to acknowledge the assistance of Dan Jaeger for providing the postmortem retrievals and tissue from the SUNY Upstate Anatomical Gift Program and Caitlin Pray for assistance with specimen testing.

References

1. Kurtz SM, Ong KL, Lau E, et al. International survey of primary and revision total knee replacement. Int Orthop. 2011
2. Bourne RB, Chesworth BM, Davis AM, et al. Patient satisfaction after total knee arthroplasty: who is satisfied and who is not? Clin Orthop Relat Res. 2010; 468:57–63. [PubMed: 19844772]
3. Weinstein AM, Rome BN, Reichmann WM, et al. Estimating the burden of total knee replacement in the United States. J Bone Joint Surg Am. 2013; 95:385–392. [PubMed: 23344005]
4. Kurtz SM, Ong KL, Schmier J, et al. Future clinical and economic impact of revision total hip and knee arthroplasty. J Bone Joint Surg Am. 2007; 89(Suppl 3):144–151. [PubMed: 17908880]
5. Furnes, O.; Espehaug, B.; Lie, S., et al. Prospective studies of hip and knee prostheses: The Norwegian Arthroplasty Register 1987–2004. American Academy of Orthopaedic Surgeons; Washington, DC: 2005. p. SE024
6. Ritter MA, Herbst SA, Keating EM, et al. Radiolucency at the bone-cement interface in total knee replacement. The effects of bone-surface preparation and cement technique. J Bone Joint Surg Am. 1994; 76:60–65. [PubMed: 8288666]
7. Li MG, Nilsson KG. Changes in bone mineral density at the proximal tibia after total knee arthroplasty: a 2-year follow-up of 28 knees using dual energy X-ray absorptiometry. J Orthop Res. 2000; 18:40–47. [PubMed: 10716277]
8. Lonner JH, Klotz M, Levitz C, et al. Changes in bone density after cemented total knee arthroplasty: influence of stem design. J Arthroplasty. 2001; 16:107–111. [PubMed: 11172279]
9. Li MG, Nilsson KG. No relationship between postoperative changes in bone density at the proximal tibia and the migration of the tibial component 2 years after total knee arthroplasty. J Arthroplasty. 2001; 16:893–900. [PubMed: 11607906]
10. Mann KA, Miller MA, Pray CL, et al. A new approach to quantify trabecular resorption adjacent to cemented knee arthroplasty. J Biomech. 2012; 45:711–715. [PubMed: 22227315]
11. Miller MA, Goodheart JR, Izant TH, et al. Loss of Cement-bone Interlock in Retrieved Tibial Components from Total Knee Arthroplasties. Clin Orthop Relat Res. 2014; 472:304–313. [PubMed: 23975251]
12. Race A, Miller MA, Clarke MT, et al. The effect of low-viscosity cement on mantle morphology and femoral stem micromotion: A cadaver model with simulated blood flow. Acta Orthop. 2006; 77:6007–6616.
13. Mann KA, Miller MA, Race A, et al. Shear fatigue micromechanics of the cement-bone interface: An in vitro study using digital image correlation techniques. J Orthop Res. 2009; 27:340–346. [PubMed: 18846550]

14. Shaffer JP. Multiple hypothesis testing. Annu Rev Psychol. 1995; 46:561–584.
15. Chen H, Washimi Y, Kubo KY, et al. Gender-related changes in three-dimensional microstructure of trabecular bone at the human proximal tibia with aging. Histol Histopathol. 2011; 26:563–570. [PubMed: 21432771]
16. Taylor M, Tanner KE, Freeman MA. Finite element analysis of the implanted proximal tibia: a relationship between the initial cancellous bone stresses and implant migration. J Biomech. 1998; 31:303–310. [PubMed: 9672083]
17. Krause WR, Krug W, Miller J. Strength of the Cement-Bone Interface. Clin Orthop. 1982; 163:290–299. [PubMed: 7067264]
18. Askew MJ, Steege JW, Lewis JL, et al. Effect of cement pressure and bone strength on polymethylmethacrylate fixation. J Orthop Res. 1984; 1:412–420. [PubMed: 6491790]
19. Majkowski RS, Miles AW, Bannister GC, et al. Bone surface preparation in cemented joint replacement. J Bone Jnt Surg. 1993; 75-B:459–463.
20. Mann KA, Ayers DC, Werner FW, et al. Tensile strength of the cement-bone interface depends on the amount of bone interdigitated with PMMA cement. J Biomech. 1997; 30:339–346. [PubMed: 9075001]
21. Waanders D, Janssen D, Mann KA, et al. The mechanical effects of different levels of cement penetration at the cement-bone interface. J Biomech. 2010; 43:1167–1175. [PubMed: 20022010]
22. Gebert de Uhlenbrock A, Puschel V, Puschel K, et al. Influence of time in-situ and implant type on fixation strength of cemented tibial trays - a post mortem retrieval analysis. Clin Biomech (Bristol, Avon). 2012; 27:929–935.
23. Breer S, Krause M, Busse B, et al. Analysis of retrieved hip resurfacing arthroplasties reveals the interrelationship between interface hyperosteoidosis and demineralization of viable bone trabeculae. J Orthop Res. 2012; 30:1155–1161. [PubMed: 22180341]
24. Mann KA, Miller MA. Fluid-structure interactions in micro-interlocked regions of the cement-bone interface. Comput Methods Biomech Biomed Engin. 2013 In Press.
25. Lu JX, Huang ZW, Tropiano P, et al. Human biological reactions at the interface between bone tissue and polymethylmethacrylate cement. J Mater Sci Mater Med. 2002; 13:803–809. [PubMed: 15348569]
26. Walker PS, Soudry M, Ewald FC, et al. Control of cement penetration in total knee arthroplasty. Clin Orthop Relat Res. 1984:155–164. [PubMed: 6705374]

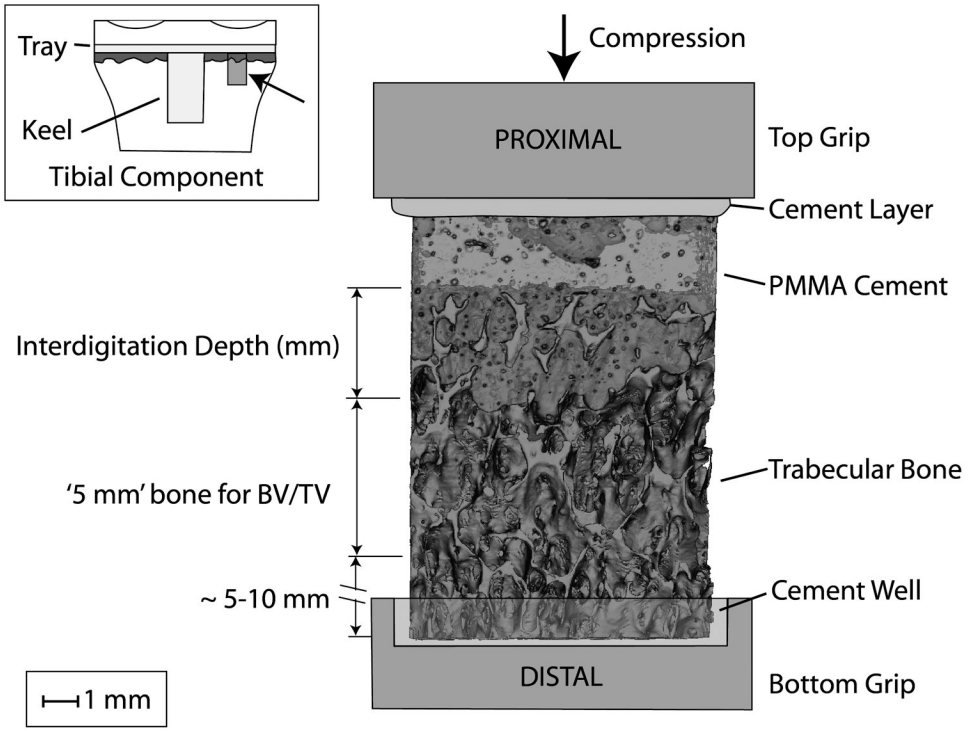

Figure 1.

Experimental set-up for mechanical testing of the cement-bone interface from the tibial tray of knee replacements. The inset figure shows (arrow) example of procurement location of test sample below the tibial tray. The interdigitation depth of cement penetration into trabecular bone and the 5 mm region where trabecular bone morphology measurements were made are shown.

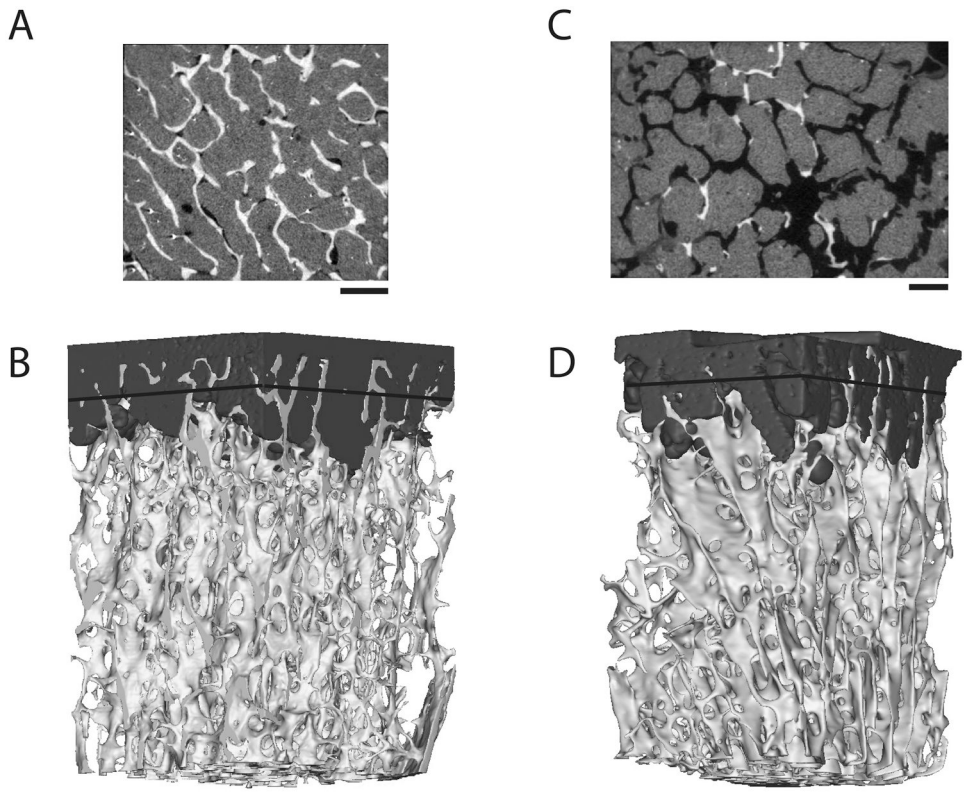

Figure 2.

MicroCT trans-axial section (**A**) and a full reconstruction (**B**) of a freshly-cemented specimen (FC3) illustrating good interlock between the cement and bone. The location of the trans-axial cut is indicated by a black line in panel B. A postmortem specimen (PM4) had extensive bony resorption in the interdigitated region (**C–D**). In the trans-axial images (A and C), the trabeculae are white, cement is gray, and voids or spaces are black. A 1mm bar scale is shown.

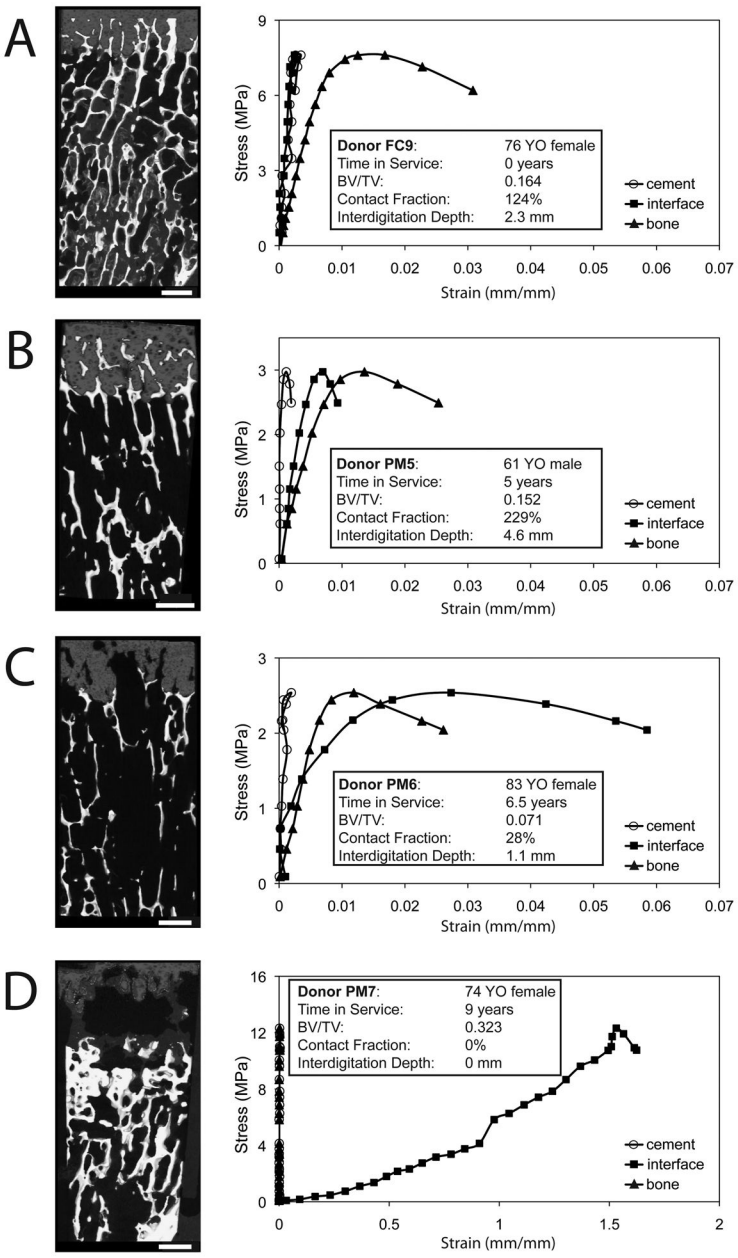

Figure 3.

Stress-strain response ascribed to the cement, cement-bone interface, and trabecular bone for loading in compression. Examples are shown for a freshly-cemented construct (**A**), postmortem retrievals with substantial remaining interlock (**B**) and near-full loss of (**C**) cement-bone interlock, and a case with a large cement-bone gap with fibrous tissue formation (**D**). Reconstructed images at the specimen faces were created to illustrate the general morphology for each specimen. Interface displacement measurements are presented as strain assuming a gage length of 1mm.

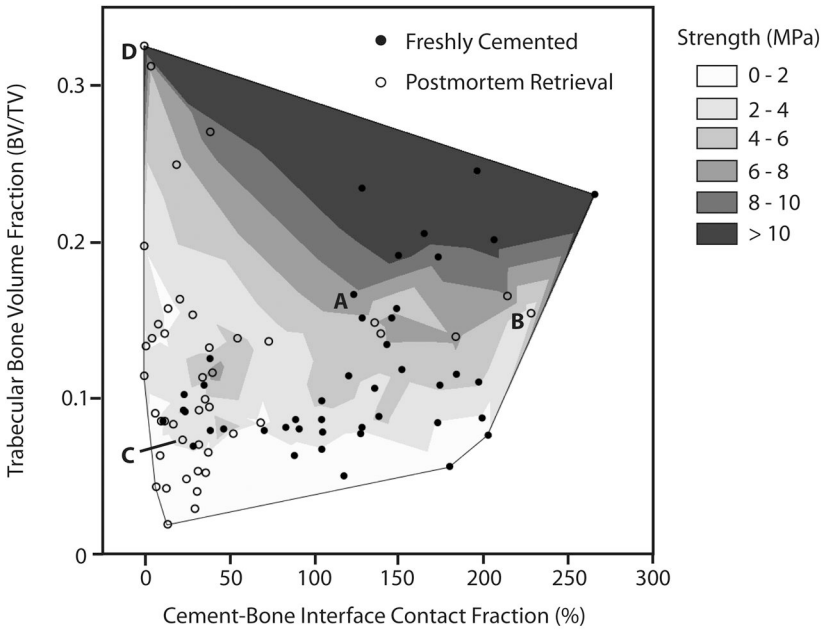

Figure 4.

Contour plot of cement-bone compression strength as a function of interface contact fraction and bone volume fraction for freshly-cemented (filled circles) and postmortem retrieved specimens (open circles). The data points designated A to D correspond to frames A to D in Figure 3. Specimens with more cement-bone contact fraction and greater supporting bone volume fraction had higher compressive strength.

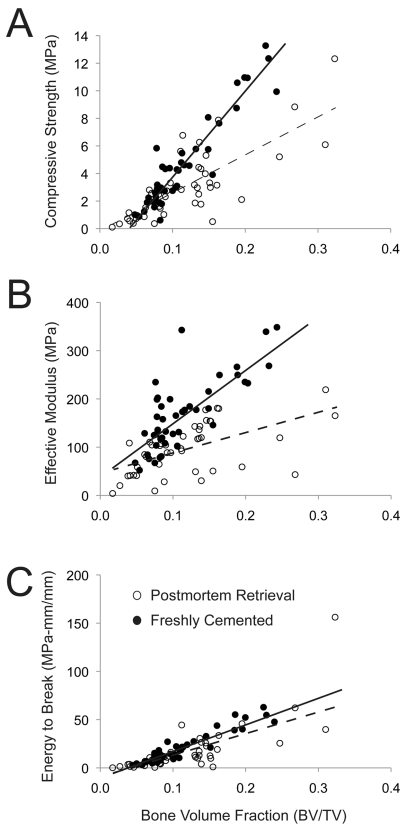

Figure 5.

Compressive strength (**A**), effective modulus (**B**), and energy to failure (**C**) for cement-bone specimens are shown as a function of supporting trabecular bone volume fraction (BV/TV) and source (postmortem retrieval and freshly-cemented). Linear regression lines are shown for the postmortem retrieval (dashed) and freshly-cemented (solid) cases.

Table 1

Eleven freshly-cemented tibial components (created in the lab) and eleven postmortem retrievals were used to generate cement-bone test specimens used for morphological assessment and mechanical testing. One donor (PM1 and PM2) had bilateral implants. A mock metal tray was used to press the cement into the bone bed for FC3-FC11.

Freshly- cemented (FC) or Postmortem retrieval (PM)	Time in service (years)	Sex	Age (years)	BMI (kg/m^2)	Cause of Death	Manufacturer: Type	Stem (S) or Stem with Keel (SK)	Cruciate Retaining (CR) or Posterior Stabilized (PS)
FC1	0	M	70	34.3	Cardiorespiratory Arrest	Stryker: Triathlon	SK	CR
FC2	0	F	67	36.4	Acute MI	Stryker: Scorpio	SK	PS
FC3	0	F	81	26.0	Cardiac Arrest	Mock metal tray	None	N/A
FC4	0	F	90	26.3	Cardiac Arrest	Mock metal tray	None	N/A
FC5	0	F	63	22.6	Cerebral Vascular Injury	Mock metal tray	None	N/A
FC6	0	F	83	35.7	Lung Cancer	Mock metal tray	None	N/A
FC7	0	F	85	34.6	Cardiopulmonary Arrest	Mock metal tray	None	N/A
FC8	0	F	91	16.9	Cardiorespiratory Failure	Mock metal tray	None	N/A
FC9	0	F	76	30.0	Metastatic Lung Cancer	Mock metal tray	None	N/A
FC10	0	M	64	23.9	Cardiopulmonary Arrest	Mock metal tray	None	N/A
FC11	0	F	75	31.4	Cardiopulmonary Arrest	Mock metal tray	None	N/A
PM1	1	F	73	22.7	Cardiopulmonary Arrest	Biomet: Vanguard	SK	CR
PM2	2	F	73	22.7	Cardiopulmonary Arrest	Biomet: Vanguard	SK	CR
PM3	2.5	F	82	36.5	Congestive Heart Failure	Depuy: PFC Sigma	SK	PS
PM4	3	F	84	24.1	Pulmonary Infection - Sepsis	Zimmer: Nexgen	SK	PS
PM5	5	M	61	36.3	Cardiopulmonary Arrest	Stryker: Triathlon	SK	CR
PM6	6.5	F	83	23.7	Carcinoma	Stryker: Scorpio	SK	PS
PM7	9	F	74	31.9	Renal Failure - Cardiac Arrest	Zimmer: Nexgen	SK	PS
PM8	10	M	78	18.4	Pick’s Disease	Depuy: AMK	S	PS
PM9	11	F	69	22.5	Rectal Cancer	Wright Medical: Advanced	SK	PS
PM10	16	F	65	31.4	Cardiopulmonary Arrest	Strkyer: Duracon	SK	CR
PM11	20	F	90	23.2	Cardiopulmonary Arrest	Zimmer: Insall Burstein I	S	PS

Table 2

Morphology parameters describing cement-bone interlock include the contact fraction and interdigitation depth. Morphology parameters for the trabecular bone adjacent to the cement-bone interface include bone volume fraction (BV/TV), connectivity density (Conn.D), structural model index (SMI), trabecular thickness (Tb.Th), trabecular spacing (Tb.Sp), degree of anisotropy (DA), and tissue density.

Morphology Parameter	Freshly Cemented Mean (sd) [range] (n=44)	Postmortem Mean (sd) [range] (n=44)	Corrected P-value
Contact fraction (%)	121 (61) [11.1 – 267]	42 (55) [0 – 229]	0.0008
Interdigitation Depth (mm)	2.9 (0.8) [1.0 – 4.1]	1.8 (1.3) [0.0 – 4.6]	0.0008
BV/TV	0.113 (0.051) [0.048 – 0.243]	0.118 (0.069) [0.017 – 0.323]	0.736
Conn.D (1/mm)	4.13 (1.24) [2.02 – 7.12]	4.00 (1.91) [0.66 – 8.47]	0.736
SMI	1.67 (0.49) [0.29 – 2.33]	1.82 (0.52) [0.36 – 2.88]	0.531
Tb.Th (mm)	0.131 (0.022) [0.096 – 0.189]	0.145 (0.045) [0.091 – 0.293]	0.348
Tb.Sp (mm)	0.80 (0.14) [0.49 – 1.15]	0.89 (0.28) [0.56 – 1.89]	0.348
DA	1.91 (0.38) [1.15 – 2.75]	1.78 (0.40) [1.17 – 2.60]	0.348
Tissue Density (mm/cc HA)	1017 (26.4) [935 – 1079]	1000 (34.6) [922 – 1086]	0.079

Table 3

A regression model with compressive strength of the cement-bone interface as the dependent variable and cement-bone interface contact fraction (CF) and supporting trabecular bone volume fraction (BV/TV) as independent variables was performed. Specimens with greater BV/TV and greater CF had greater compressive strength. Postmortem retrieval specimens and freshly-cemented specimens were grouped for this analysis (n=88).

Mechanical Parameter	Summary of Fit	Morphology Parameter	Estimate	Std Error	P value
Strength (MPa)	$r^2 = 0.72$, p=0.0001	BV/TV	36.3	2.92	0.0001
		CF (%)	1.4	0.25	0.0001
		Intercept	−1.49	0.002	0.0004

Table 4

Analysis of covariance (ANCOVA) models for cement-bone interface compressive strength, effective modulus and energy to break were used with supporting bone trabecular bone volume (BV/TV) and Type (PM-postmortem or FC-freshly-cemented) as independent variables. The interaction term (BV/TV * Type) was used to determine if the slopes were different for the two Types.

Mechanical Parameter	Summary of Fit	Morphology Parameter	Estimate	Std Error	P value
Strength (MPa)	$r^2 = 0.62$, p=0.0001	BV/TV	44.6	2.6	0.0001
		Type (PM or FC)	0.87	0.15	0.0001
		BV/TV*Type	15.9	2.6	0.0001
		Intercept	−1.27	0.33	0.0003
Effective Modulus (MPa)	$r^2 = 0.65$, p=0.0001	BV/TV	774	85	0.0001
		Type (PM or FC)	37.2	4.9	0.0001
		BV/TV*Type	358.5	85.2	0.0001
		Intercept	43.1	10.9	0.0002
Energy to Break (MPa-mm/mm)	$r^2 = 0.66$, p=0.0001	BV/TV	287	23.3	0.0001
		Type (PM or FC)	1.78	1.34	0.188
		BV/TV*Type	11.2	23.4	0.63
		Intercept	−14.2	3.0	0.0001